CONF-890561--1

SAND--88-1583C

TI89 003141

NOV 14 1988

# Stress Analysis of the Liner and Liner Anchorage System Near Penetrations in a Reinforced Concrete Reactor Containment

J. Randall Weatherby[1]

An overpressurization experiment was conducted on a scale–model of a reinforced concrete containment building. The test was terminated when tears formed in the steel liner. Virtually all leakage occurred through a large tear that propagated along the edge of a thickened insert plate that surrounded a piping penetration. This paper describes the results of a post–test finite element analysis of this region. Results of the analysis indicate that the large tear initiated due to high strains produced by a stud anchor. The results of the analysis also suggest that a relatively simple analytical technique can be used to estimate the pressure at which tears will initiate near penetrations in lined containment structures.

## Introduction

Sandia National Laboratories has conducted an overpressurization experiment on a 1:6-scale model of a reinforced concrete containment building. The program, which was sponsored by the U. S. Nuclear Regulatory Commission, is part of an ongoing effort to develop test-validated methods for assessing the performance of light water reactor containment buildings under severe accident loads. Several organizations submitted analytical predictions of the structural response of the 1:6-scale model before the overpressurization test was conducted (Clauss, 1987). By comparing the measured response to the predictions, much has been learned about the accuracy of the modeling assumptions applied in these analyses. More importantly, the test has revealed at least one set of structural details and mechanisms that can control the failure mode of containment buildings made of reinforced concrete.

During the experiment, numerous cracks or tears formed in the steel liner which served as the pressure boundary for the structure. When the pressure inside the model reached 145 psig, leakage through tears in the liner became so large that the pressure could not be increased further. Virtually all leakage occurred through a single tear that initiated near the edge of a thickened insert plate that surrounds a series of three pipes which penetrate the containment wall. The tear propagated along the edge of the plate through a distance of 22 inches before arresting (see Figure 1). The insert plate has a nominal thickness of 3/16 of an inch while the surrounding liner is 1/16 of an inch thick.

Post-test finite element analyses of this region have been conducted to study and isolate the mechanism(s) responsible for the initiation of the tear. The results of the present investigation strongly suggest that the tear formed as the result of strain concentrations that developed at the base of studs that were used to anchor the liner to the concrete wall of the containment. Important factors that lead to these strain concentrations were: (1.) slippage between the

[1]Member of Technical Staff, Applied Mechanics Division I, Sandia National Laboratories, Albuquerque, NM 87185.

---

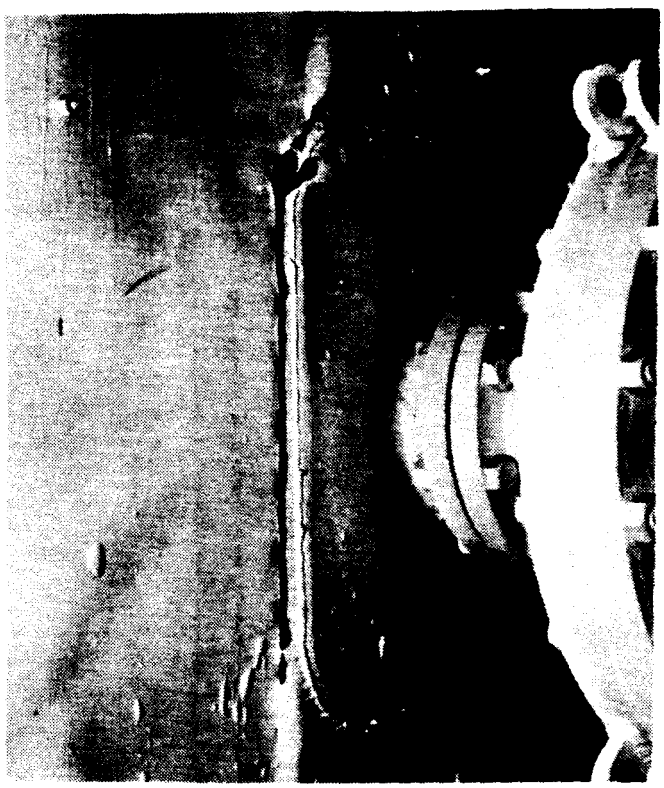

Figure 1: The 22-Inch Liner Tear Located Near a Piping Penetration

liner and concrete induced by the thickened insert plate, and (2.) the point-wise restraint against slip provided by the stud anchors. In the analysis, the liner strains in elements adjacent to studs located near the insert plate reached magnitudes sufficient to cause liner tearing at an internal pressure somewhere between 143 and 148 psig. Although this pressure range is fairly narrow, the maximum principal strains next to the stud anchors increase so rapidly that a large uncertainty in the failure criterion for tear initiation translates into a very small uncertainty in the internal pressure at the point of tear initiation.

## The Liner Anchorage System

The liner and insert plate are anchored to the concrete wall by headed studs. The purpose of the anchorage system is to prevent buckling of the liner if the liner is exposed to high temperatures (for example, a case where a broken steam line sprays hot steam on the liner). In the 1:6-scale model, the studs were welded to the outer surface of the liner and insert plate in a square grid pattern as shown in Figure 2. As the concrete wall was cast, the heads and shanks of the studs were embedded in the concrete.

Each stud in Figure 2 is 3/4 inches in length and has a shank diameter of 0.135 inches. On the liner near the insert plate and on the insert plate itself, the studs were placed with a 2 inch $\times$ 2 inch spacing. Away from the insert plate, the spacing changes to 6 inch $\times$ 6 inch. The column of studs on the liner nearest to the insert plate was located approximately 0.5 inches from the edge of the insert plate.

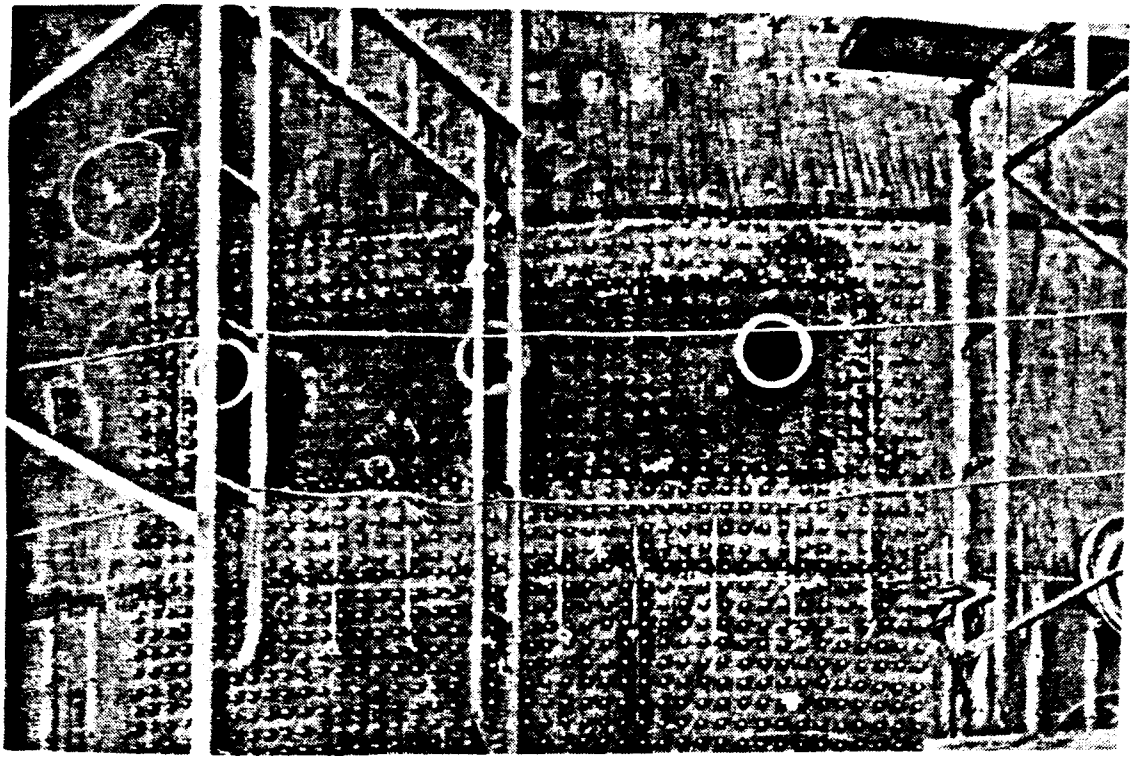

Figure 2: Arrangement of the Studs Near the Piping Penetration

Mechanics of Liner Tearing

Idealizations are made in all models used in the analysis of complex structures. Such idealizations are necessary to limit the size and complexity of the analysis and to conform to the modeling tools available to the analyst. As a result, the response of an analytical model will always deviate from the response of the real structure. Problems arise when details that lead to failure of the structure are excluded from consideration by simplifying assumptions made in the analysis. This proved to be a problem in predicting the failure mode and ultimate pressure capacity of the 1:6-scale containment model. Post-test inspections of the model revealed that all liner tears occurred next to stud anchors. The liner anchorage system, which apparently played a key role in the initiation of liner tearing, was not modeled in any of the pretest analyses of the 1:6-scale model (Clauss, 1987). What follows is a brief explanation of the events that caused the 22-inch tear to initiate near the piping penetration.

At locations in the cylinder far away from piping penetrations, equipment hatches, and other discontinuities, the load carried by the studs was probably very small. Any deviation from zero load was the result of non-uniform deformations in the wall resulting from cracks in the concrete. Near the piping penetration, however, the situation was significantly different. The insert plate, because of its greater thickness, was stiffer than the surrounding liner and tended to stretch much less. As a result, the studs on and immediately surrounding the insert plate were put into shear as they attempted to force the insert plate to follow the vertical and circumferential expansion of the reinforced concrete wall. The highly concentrated forces from the studs produced large strains in the liner near the insert plate eventually causing the liner to tear. Further away from the insert plate, where the stud forces were small, the

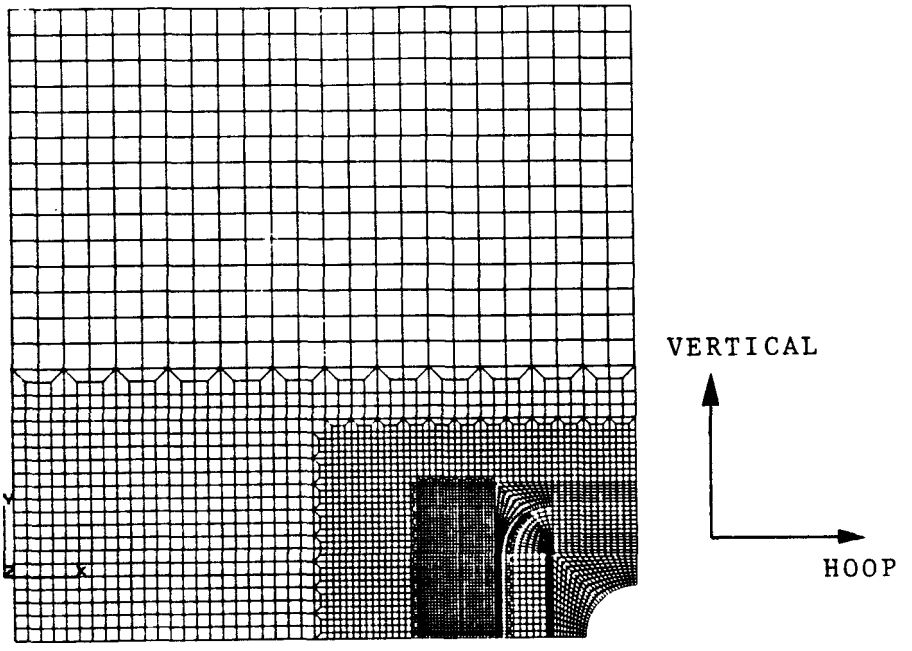


Figure 3: Plane Stress Finite Element Model of the Region Surrounding the Piping Penetration

strains in the liner were more like those that would exist in a long, uniform cylinder.

Finite Element Model of the Penetration Region

The 1:6-scale model experiment has shown that the liner anchorage system is one detail that cannot be ignored in analyses aimed at predicting the failure mode of reinforced concrete containment buildings loaded by internal pressure. The purpose of this analysis of the piping penetration was to determine how stud forces develop and if simple techniques can be used to estimate the magnitude of strains in the vicinity of the studs.

Figure 3 shows the plane stress finite element model that was constructed to analyze the region surrounding the piping penetration. ABAQUS, a general purpose finite element code, was used for this investigation. The liner and insert plate were modeled using 4-node bilinear quadrilateral elements. Each stud was modeled using a discrete spring element which has the property that the line of action of the force in the element is parallel to the line segment joining the two nodes at each end of the element. The analysis was run using the nonlinear geometry option to account for finite strains.

Because the studs are modeled with spring elements, they introduce point loads into the mesh of quadrilateral elements. For this reason, the dimensions of the quadrilateral elements are crucial. As the mesh is refined, the strains for a given value of internal pressure will increase without bound in those quadrilateral elements that are connected to springs. In the real structure, the stud forces are introduced over an area roughly equal to the cross-sectional area of the

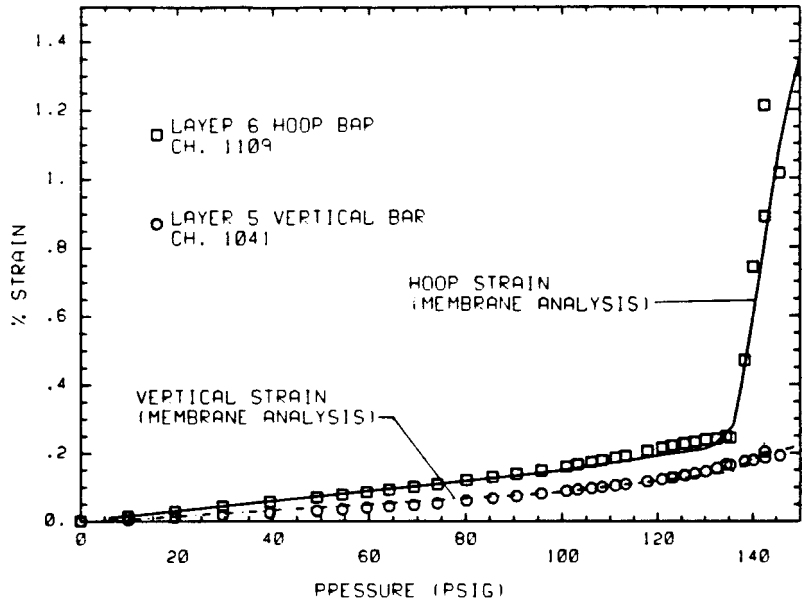


Figure 4: Comparison of Measured and Calculated Strains in the Hoop and Vertical Directions. Calculated Values are Taken From the Infinite Cylinder Analysis. Measured Values are Taken From Gages on Hoop and Vertical Rebars Located Behind the Insert Plate.

stud shank. Therefore, to avoid unrealistically high strains in the analysis, the minimum length of an element side should not be less than half the diameter of the stud shank. The smallest elements in the model are located between the first column of studs on the liner and the edge of the insert plate. Here, each element is 0.25 inches in length in the vertical direction, and 0.1 inches in length in the horizontal direction. Both dimensions are less than the stud radius (0.0675 in).

In this calculation, the reinforced concrete wall was not modeled; instead, the motion of the wall was assumed to be identical to that of an infinite cylinder with a 1/16-inch thick liner and the same vertical, hoop, and seismic reinforcement as found in the midsection of the 1:6-scale model. The infinite cylinder analysis was described in (Weatherby, 1987) and assumed that all load was carried by the rebar and liner; no tensile strength was attributed to the concrete. Assuming that the strains in the wall are uniform is equivalent to assuming that the amount of load transferred between the wall and insert plate via the anchorage system is negligible when compared to the vertical and horizontal loads carried by the reinforcement at a given internal pressure. As shown in Figure 4, the strains calculated in the infinite cylinder analysis were found to be in close agreement with the actual strains measured in hoop and vertical reinforcing bars located behind the insert plate. This supports the idea that the deformation of the wall is not significantly affected by the presence of the thickened insert plate.

The boundary conditions applied to the edges of the model are listed in Table 1. In this table, a *no-slip* boundary condition in a particular direction implies that the liner is forced to follow the motion of the wall in that direction. For example, a no-slip boundary condition in the hoop direction implies that the displacement

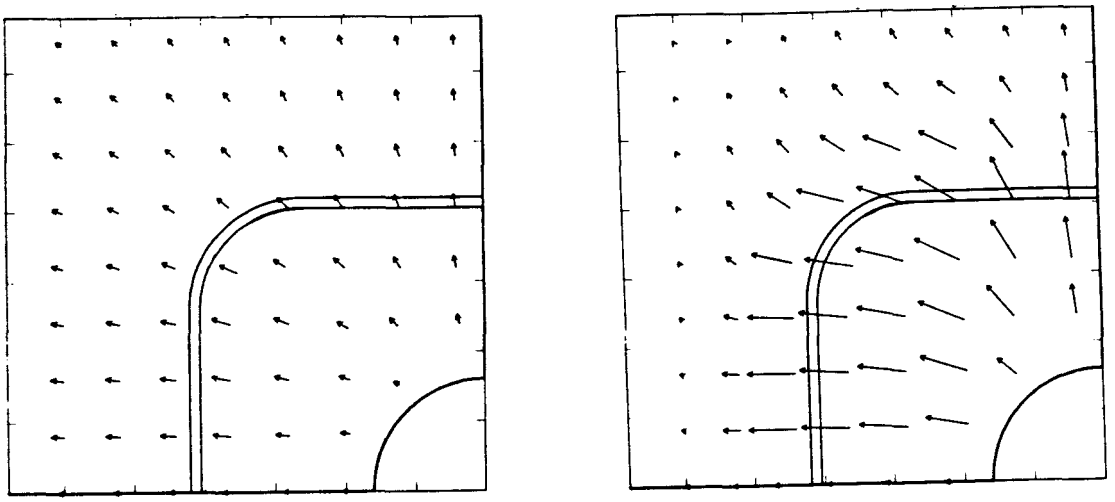


Figure 5: Magnitudes and Directions of the Forces Exerted by the Studs on the Insert Plate and Liner

Analytical Results

As the containment wall deforms, forces develop in the studs as they attempt to force the stiff insert plate to follow the motion of the wall. The vector plots in Figure 5 show the relative magnitudes and directions of the forces that studs in the vicinity of the piping penetration exert on the liner and insert plate at 75 psig and 145 psig. Figure 6 shows in more detail how the stud forces vary as a function of internal pressure. In general, the forces in the first column of studs adjacent to the insert plate increase until reaching a local maximum at approximately 70 psig internal pressure. This corresponds to the pressure when the liner begins to yield locally around the first column of studs. The forces in studs S1 through S4 begin to increase again at 90 psig, and continue to rise until reaching a maximum of approximately 1400 lb at 145 psig internal pressure. Above this pressure, the stud force begins to rapidly decrease. This second region of decreasing stud force begins when the elements connected to studs S1 through S4 reach 15% equivalent plastic strain, which is the point where it is assumed that the liner material ceases to work-harden.

A contour plot of the maximum principal strain in the liner at 145 psig is shown in Figure 7. Along the straight, vertical segment of the insert plate boundary, the contours are virtually symmetric about horizontal lines that pass through the studs and about horizontal lines that pass halfway between the studs. The largest principal strains were reached in the elements connected to studs S1 through S4. The values of the maximum principal strain are approximately equal in those elements that are connected to studs S1, S2, and S3. The principal strains next to the fourth stud (S4) are slightly higher than the strains next to the first three studs making this the most likely site for tear initiation.

Table 1: Boundary Conditions Applied to the Finite Element Model

| Boundary | Boundary Condition | |
|---|---|---|
| | Hoop Direction | Vertical Direction |
| Left Edge | no-slip | no-traction |
| Right Edge | no-slip | no-traction |
| Top Edge | no-traction | no-slip |
| Bottom Edge | no-traction | no-slip |
| Pipe Edge | no-slip | no-slip |

in the hoop direction is given by

$$u_h = x\,\epsilon_h \tag{1}$$

where $u_h$ is the displacement in the hoop direction, $x$ is the circumferential distance from the center of the pipe at the lower right corner of the finite element model, and $\epsilon_h$ is the strain in the hoop direction given by the infinite cylinder analysis.

An approximate load–deflection curve was constructed for the studs based on data obtained from shear tests performed on studs embedded in concrete (Horschel, 1988). Initially, both nodes on each spring element occupied the same location in the finite element model. One node on each spring was connected to either the liner or the insert plate. During the analysis, the motion of the second node on each spring was specified to follow the motion of the containment wall as determined from the infinite cylinder analysis.

Liner Material Properties

A number of uniaxial tensile tests were conducted to determine the material properties of the liner and insert plate. The liner is made of A414 Grade D steel while the insert plate is made of A516 Grade 60 steel. Both materials have a yield strength of approximately 50 ksi. Both the A414 steel and the A516 steel show considerable strain hardening after yielding. The A414 steel reaches a true stress of 82 ksi at maximum load while the A516 steel exhibits slightly more hardening and reaches a true stress of approximately 92 ksi at maximum load. A total of four uniaxial tensile tests were conducted on the liner material: two in the rolling direction, and two in the transverse direction. The elongations at fracture were 21.3% and 30.0% in the rolling direction and 39.1% and 27.8% in the transverse direction (Knorovsky, *et al*, 1988).

In the finite element analysis, a piecewise linear relationship was used to define the stress–plastic strain curves of the two steels. The hardening of both materials was assumed to be zero when the equivalent plastic strain exceeded 15%. This is the strain level when maximum load was reached in uniaxial tensile tests on both materials.

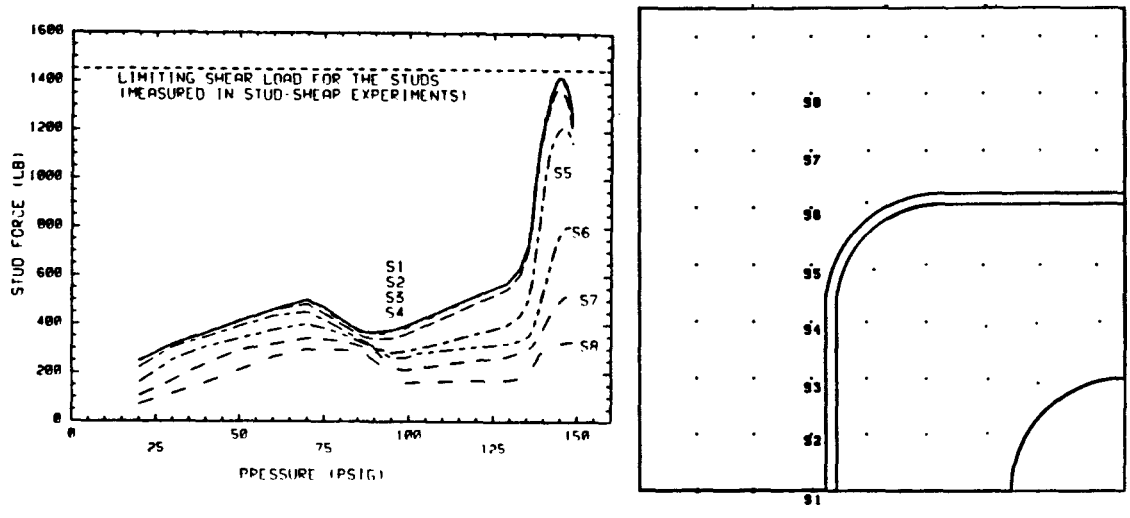


Figure 6: Stud Forces Acting on the Liner as a Function of Internal Pressure

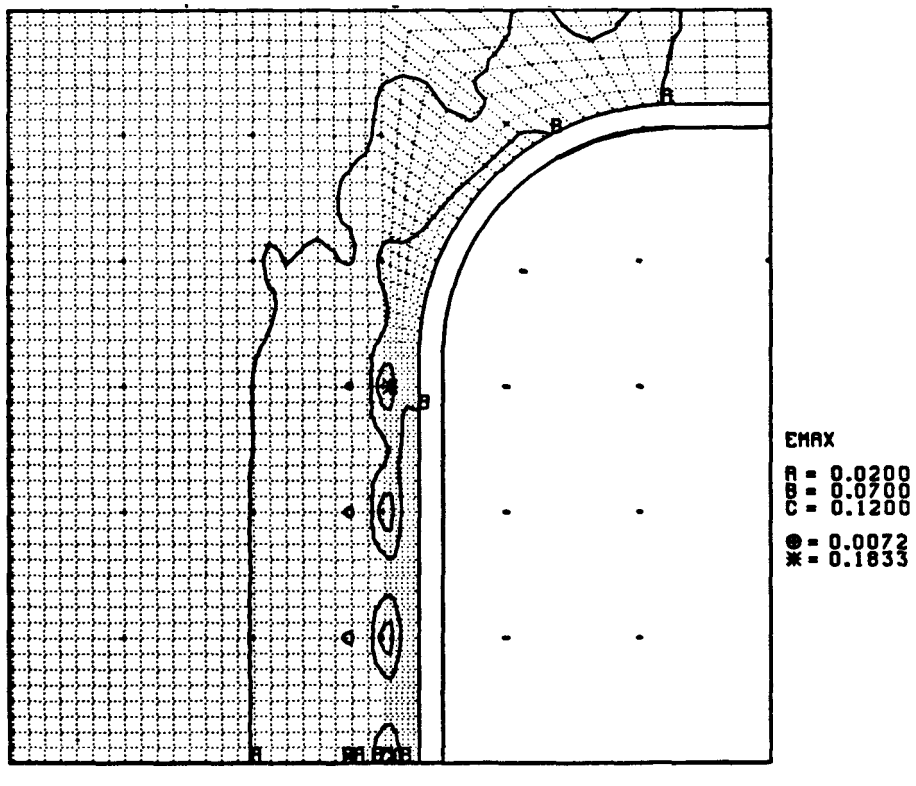


Figure 7: Maximum Principal Strains in the Liner at 145 Psig Internal Pressure

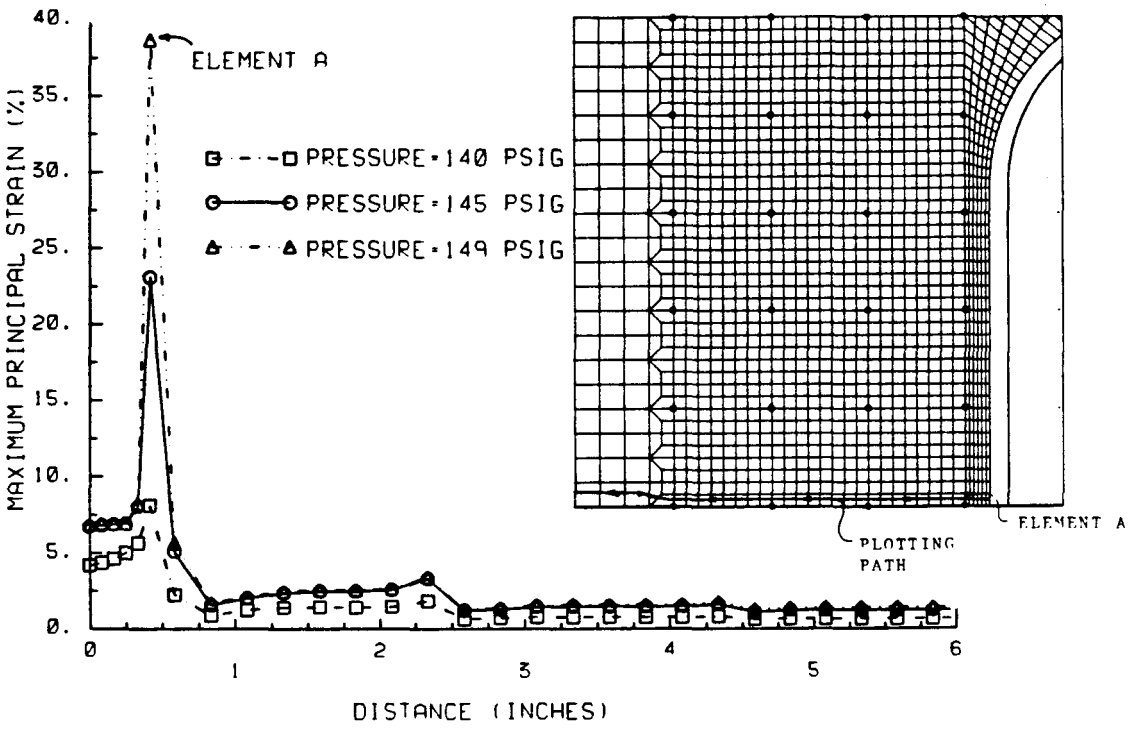


Figure 8: Maximum Principal Strain in the Liner as a Function of Distance From the Edge of the Insert Plate. Abrupt Changes in Strain Mark the Location of Studs.

As the pressure increases, strains became increasingly localized in elements connected to the first column of studs. Figure 8 shows the maximum principal strain plotted as a function of position in the first row of quadrilateral elements next to the lower boundary of the mesh. In these plots, abrupt changes in strain clearly mark the location of each stud. Above 140 psig, the strain increases many times faster in Element *A* than in the other elements. Element *A* is connected to the liner stud that is closest to the insert plate.

The strains calculated in the analytical model were compared against an empirically-based fracture criterion developed by Manjoine (Manjoine, 1982). Based on this fracture criterion and the calculated strains, the liner would begin to tear near the stud anchors at 143 psig. By 148 psig, the maximum principal strains in the liner near the stud anchors exceeded the strain at fracture measured in uniaxial tension tests of the liner material.

## Conclusions

A finite element analysis of the liner surrounding a piping penetration in the 1:6-scale model has been described. Based on this investigation and post-test inspections of the model the following conclusions may be drawn:

- Forces introduced by the stud anchors caused the initiation of the 22-inch liner tear. The stud forces that caused the tear developed as the result of slippage between the liner and the reinforced concrete wall.

- The tear initiated at one of the stud anchors in the first column of studs next to the insert plate. The state of strain is virtually the same around each of the first four studs in this column so that it is hard to say which stud was the site where the tear initiated. Strains in the fourth stud up from the horizontal mid–plane are slightly higher than the strains next to the first three studs in this column.

- At the failure point, the regions of high strain (> 15%) were very small in size and confined to the material immediately surrounding the studs. The analysis as well as visual observations and thickness measurements support this conclusion.

- When an empirically-based failure criterion is used in conjunction with the finite element analysis, liner tearing is predicted to occur at approximately 143 psig internal pressure. The maximum value of internal pressure achieved in the experiment was 145 psig. Because the maximum strains increased rapidly in the analysis, any reasonable strain–based criterion of failure would predict liner tearing by 148 psig.

Acknowledgement

This work was supported by the U. S. Nuclear Regulatory Commission and performed at Sandia National Laboratories which is operated for the U. S. Department of Energy under Contract Number DE-AC04-76DP00789.

Appendix I. – References

1. Clauss, D. B., (ed.), *Round Robin Pretest Analyses of a 1:6-Scale Reinforced Concrete Containment Model Subject to Static Internal Overpressurization*, NUREG/CR-4913, SAND87- 0891, April, 1987.

2. Horschel, D. S., *Design, Construction, and Instrumentation of a 1/6-Scale Reinforced-Concrete Containment Building*, NUREG/CR-5083, SAND88-0030, August, 1988.

3. Knorovsky, G. A., Hatch, P. W.,and Gutierrez, M. R., *Evaluation of Materials of Construction for the Reinforced Concrete Reactor Containment Model*, NUREG/CR-5099, SAND88-0052, September, 1988.

4. Manjoine, M. J., "Creep-Rupture Behavior of Weldments," *Welding Journal*, Vol. 61, No. 2, February, 1982, p. 50.

5. Weatherby, J. R., "SNL Pretest Analyses," in *Round Robin Pretest Analyses of a 1:6-Scale Reinforced Concrete Containment Model Subject to Static Internal Overpressurization*, Clauss, D. B., (ed.), NUREG/CR-4913, SAND87-0891, April, 1987, pp. 40-81.

Appendix II. – Unit Conversions

| | | |
|---|---|---|
| 1 inch (in.) | = | 25.4 millimeters (mm) |
| 1 pound (lb) | = | 4.45 Newtons (N) |
| 1 pound per square inch (psi) | = | $6.89 \times 10^3$ Pascals (Pa) |